Exact Synthesis and Implementation of New High-Order Wideband Marchand Baluns

Jhe-Ching Lu, Chung-Chieh Lin, and Chi-Yang Chang, *Member, IEEE*

***Abstract*—New ultra-wideband high-order Marchand baluns with one microstrip unbalanced port and two microstrip balanced ports are proposed in this paper. The proposed Marchand baluns are synthesized based on an S-plane high-pass prototype using the Richards' transformation. The responses of the synthesized high-order Marchand baluns are exactly predicted at all real frequencies. All circuit elements are commensurate, which means the electrical lengths of all transmission line elements are a quarter-wavelength long at the center frequency. Two fifth-order Marchand baluns with reflection coefficients of −20.53 and −21.71 dB corresponding to 131% and 152% bandwidth, respectively, are synthesized and realized using the combinations of microstrip lines, slotlines, and coplanar striplines. Simulated and measured results are presented.**

***Index Terms*—Circuit transformations, high-pass prototype, Marchand balun, planar structures, synthesis, wideband.**

I. Introduction

BALUNS [1] are widely used in RF and microwave communication systems. The main feature of baluns is to transform an unbalanced signal to a balanced signal, and vice versa. Thus, baluns can be used in antenna excitations or balanced circuit topologies such as balanced mixers, push–pull amplifiers, and phase shifters. There are many types of baluns as proposed in [1]–[5]. Among the various kinds of baluns, the Marchand balun [6]–[10] is very popular because of its relatively wider bandwidth of amplitude and phase balance. Several methods to realize Marchand baluns have been proposed [6]–[16]

In design of a coupled-line Marchand balun, various analysis methods were presented. In [10] and [11], use of the relationships of the power wave in a balun to derive the scattering parameters can analyze a symmetrical Marchand balun, but the exact prediction is only valid at the center frequency. In [12], inclusion of the parameter of the electrical length of the transmission line can predict broadband performances, but the approach lacks generality. Furthermore, to achieve wider bandwidth, multiconductor coupled lines to realize tight couplings were presented. Another method is the even- and odd-mode analysis method. However, it is limited to the case of a symmetrical coupled-line Marchand balun with the maximally flat responses.

Actually, the exact synthesis of conventional Marchand baluns has been presented in [6]–[9]. A Chebyshev response can be synthesized using the synthesis method. While focusing on realizing Marchand baluns with planar coupled-line technologies, useful design values of even- and odd-mode parameters in each coupled line section are available in [9]. Nevertheless, when bandwidth of a balun is a major consideration, one should concern the limited range of practical even- and odd-mode impedance values of coupled lines.

In [17], coupled lines with suitable lumped capacitors are utilized to constitute the new miniaturized planar Marchand baluns. The circuits were synthesized based on the bandpass prototype in the Richards' domain. The key issue to use the Richard's domain bandpass prototype is to shrink the circuit size. However, the circuit in [17] may not be easy to design a wider band performance due to physical limitations of the coupled lines as described above. Moreover, the use of the capacitors to approximate the series and shunt open-circuit stubs deteriorates the wideband responses.

An interesting research on a higher order Marchand balun has been presented in [18]. The analysis of the balun is based on the chain-scattering matrices of the open-circuit series stub, short-circuited shunt stub, and uniform transmission line. With these matrices, the coefficients of the desired polynomial form describing the balun response can be numerically solved due to the formulated $N + 2$ equations, where N is equal to the element number of the balun. The stepped-impedance transformers embedded in the circuit contribute the number of order to the Marchand balun. A coplanar waveguide with a ground plane and coupled microstrip lines is used to realize the balun. The analysis method and design procedures may be complicated and the implementation of the balun occupies a relatively large circuit size.

The purpose of this paper is to propose new higher order wideband Marchand baluns and its novel implementation. The new Marchand balun structure shown in Fig. 1 is with the order higher than the conventional fourth-order Marchand balun. Compared with the conventional fourth-order Marchand baluns and their realizations, the proposed baluns have the advantages of realizable design values and very wideband performances in planar technology. During the synthesizing procedures of the Marchand Balun, one may first perform the circuit analysis on Richards' circuit elements and then obtain the prescribed characteristic functions [19], [20] to extract element values of the Marchand balun. Thus, the design of the

Manuscript received May 21, 2010; revised August 30, 2010; accepted August 31, 2010. Date of publication December 03, 2010; date of current version January 12, 2011. This work was supported in part by the National Science Council under Grant NSC98-2221-E-009-034-MY3.

J.-C. Lu is with the RF Modeling Program, Taiwan Semiconductor Manufacture Company Ltd. (TSMC), Hsinchu 300, Taiwan (e-mail: Zill_gerching@hotmail.com).

C.-C. Lin and C.-Y. Chang are with the Department of Communication Engineering, National Chiao Tung University, Hsinchu 300, Taiwan (e-mail: jack0121520@hotmail.com; mhchang@cc.nctu.edu.tw).

Color versions of one or more of the figures in this paper are available online at http://ieeexplore.ieee.org.

Digital Object Identifier 10.1109/TMTT.2010.2090702

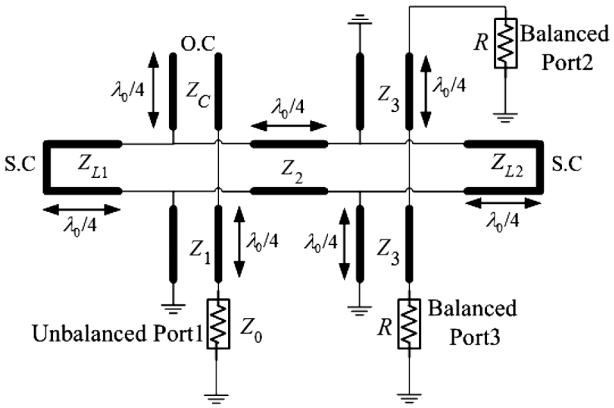

Fig. 1. Distributed circuit of the proposed fifth-order Marchand balun.

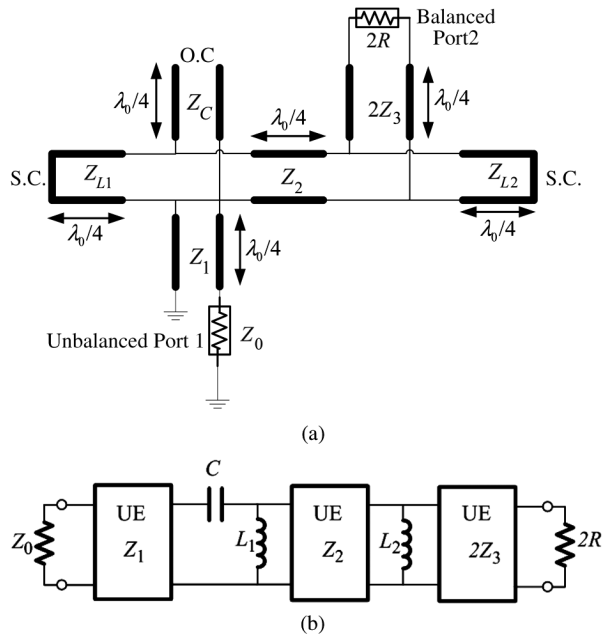

Fig. 2. Proposed fifth-order Marchand balun. (a) Two-port distributed circuit simplified in Fig. 1. (b) Its S-plane high-pass circuit.

proposed baluns is based on the S-plane high-pass prototype using Richards' transformation $S = j\tan(\pi/2(f/f_0))$, where f_0 is the center frequency of the passband, and f and S are the real frequency domain and Richards' frequency-domain variables, respectively. By applying proper circuit transformations, the proposed original distributed circuit of the Marchand balun, as shown in Fig. 1, can be converted into a fifth-order S-plane high-pass prototype, as shown in Fig. 2. With the aid of the synthesis method, all element values of the synthesized prototype can be obtained. Thus, the design parameters of the original circuit in Fig. 1 can be controlled. For realizing the balun, new combinations of the planar structures are presented for the first time. It will be shown that the microstrip lines, slot lines, and coplanar striplines are utilized to artfully implement the transmission line elements of the balun. The microstrip lines are also arranged on the other side of the slot lines, which saves the circuit area.

TABLE I
RELATIONSHIPS BETWEEN DISTRIBUTED CIRCUITS IN THE f-PLANE AND HIGH-PASS CIRCUITS IN THE S-PLANE, AND THE CORRESPONDING $ABCD$ PARAMETERS

Circuits in the f-plane	Circuits in the S-plane	ABCD Parameters
θ, Z	$C=1/Z$	$\begin{bmatrix} 1 & \frac{1}{SC} \\ 0 & 1 \end{bmatrix}$
Z, θ	$L=Z$	$\begin{bmatrix} 1 & 0 \\ \frac{1}{SL} & 1 \end{bmatrix}$
θ, Z	U.E Z	$\frac{1}{\sqrt{1-S^2}}\begin{bmatrix} 1 & ZS \\ S/Z & 1 \end{bmatrix}$

II. DERIVATION OF A FIFTH-ORDER MARCHAND BALUN

The distributed circuit of the proposed Marchand balun, as shown in Fig. 1, comprises one open-circuit series stub, two short-circuited shunt stubs, one uniform transmission line connected to input port (unbalanced port), one uniform transmission line connected to two short-circuit stubs, and two identical uniform transmission lines connected to each of the balanced output ports with impedance values corresponding to Z_C, Z_{L1}, and Z_{L2}, and Z_1, Z_2, and Z_3, respectively. The electrical lengths of all the stubs and uniform transmission lines are 90° at the center frequency. Due to differential outputs, the two output ports can be combined into one port. Thus, the two-port distributed circuit can be simplified as shown in Fig. 2(a). Its equivalent S-plane high-pass prototype is shown in Fig. 2(b). The Richards' frequency-domain variable S is defined as

$$S = j\Omega = j\tan\theta = j\tan\left(\frac{\pi f}{2f_0}\right) \tag{1}$$

where f_0 is the center frequency of the passband, and f is the real frequency domain variable. The open- and short-circuit stubs in the f-plane become a capacitor and inductors, respectively, in the S-plane. The interconnecting uniform transmission lines in the f-plane are turned into the unit elements (UEs) in the S-plane. The description of the parameters of the three important components in high-pass prototype is shown in Table I.

To derive the final fifth-order Marchand balun, circuit transformations will be used. Firstly, the circuit transformation to be used is the Kuroda's identity, as shown in Fig. 3(a) [21]. The Kuroda transformation is now applied to the shunt inductor L_1 in Fig. 2(b), thus changing the position of the shunt inductor from one side of the UE Z_2 to another side. The transformed circuit is shown in Fig. 3(b) with the following transformation equation:

$$n^2 = 1 + \frac{Z_2}{L_1}. \tag{2}$$

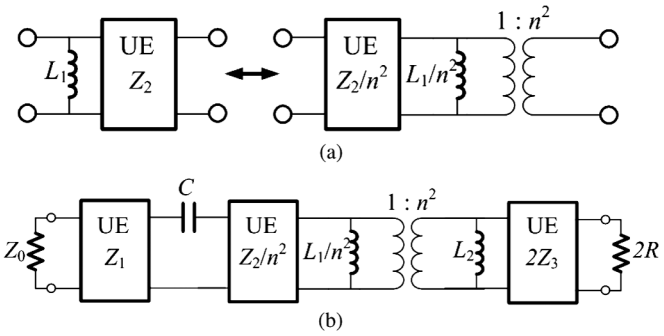

Fig. 3. First transformation. (a) Kuroda identity transformation from [21]. (b) Applying the Kuroda identity in (a) to the circuit in Fig. 2(b).

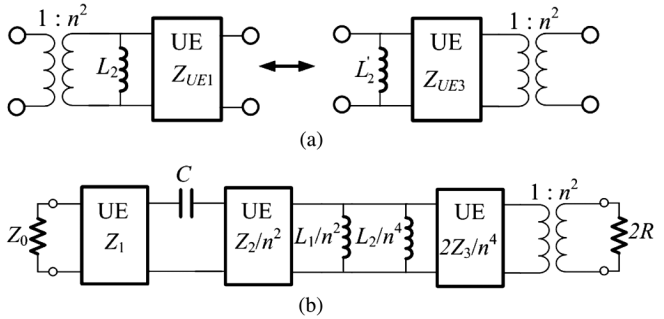

Fig. 4. Second transformation. (a) Newly presented exact circuit transformation. (b) Applying the exact circuit transformation in (a) to the circuit in Fig. 3(b).

Secondly, observation of the two shunt inductors connected by the $1:n^2$ transformer shown in Fig. 3(b) shows that one redundant shunt inductor exists. Hence, to combine the redundant element, a new circuit transformation should be derived. Consider the new circuit transformation in Fig. 4(a). The $ABCD$-parameters of the left circuit in Fig. 4(a) are

$$\frac{1}{\sqrt{1-S^2}}\begin{bmatrix}\frac{1}{n^2} & 0\\ 0 & n^2\end{bmatrix}\begin{bmatrix}1 & 0\\ \frac{1}{SL_2} & 1\end{bmatrix}\begin{bmatrix}1 & Z_{\mathrm{UE1}}S\\ \frac{S}{Z_{\mathrm{UE1}}} & 1\end{bmatrix} = \frac{1}{\sqrt{1-S^2}}\begin{bmatrix}\frac{1}{n^2} & \frac{Z_{\mathrm{UE1}}S}{n^2}\\ \frac{n^2}{SL_2}+\frac{n^2S}{Z_{\mathrm{UE1}}} & \frac{n^2Z_{\mathrm{UE1}}}{L_2}+n^2\end{bmatrix}. \quad (3)$$

The $ABCD$-parameters of the right circuit in Fig. 4(a) are

$$\frac{1}{\sqrt{1-S^2}}\begin{bmatrix}1 & 0\\ \frac{1}{SL_2'} & 1\end{bmatrix}\begin{bmatrix}1 & Z_{\mathrm{UE3}}S\\ \frac{S}{Z_{\mathrm{UE3}}} & 1\end{bmatrix}\begin{bmatrix}\frac{1}{n^2} & 0\\ 0 & n^2\end{bmatrix} = \frac{1}{\sqrt{1-S^2}}\begin{bmatrix}\frac{1}{n^2} & Z_{\mathrm{UE3}}Sn^2\\ \frac{1}{n^2SL_2'}+\frac{S}{n^2Z_{\mathrm{UE3}}} & \frac{n^2Z_{\mathrm{UE3}}}{L_2'}+n^2\end{bmatrix}. \quad (4)$$

Assume that (3) is equal to (4), the transformed parameters can be obtained as follows:

$$L_2' = \frac{L_2}{n^4}$$
$$Z_{\mathrm{UE3}} = \frac{Z_{\mathrm{UE1}}}{n^4}. \quad (5)$$

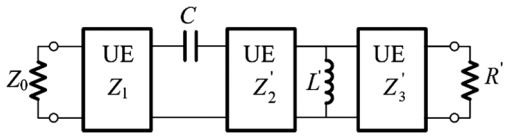

Fig. 5. Final fifth-order S-plane high-pass prototype of Marchand balun.

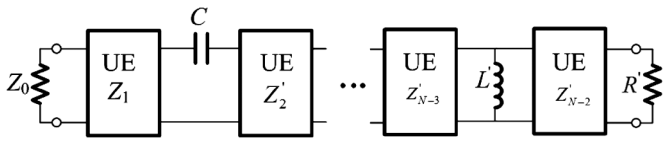

Fig. 6. N-order S-plane high-pass prototype of the Marchand balun.

Thirdly, by applying the newly derived circuit transformation, the further transformed circuit can be obtained, which is shown in Fig. 4(b). Finally, the two shunt inductors can be combined, and the $1:n^2$ transformer can be absorbed into the load resistance. Consequently, the final fifth-order Marchand balun prototype is shown in Fig. 5 with the following relations:

$$Z_2' = \frac{Z_2}{n^2} \quad (6)$$
$$L' = \frac{L_1L_2}{n^2(L_1n^2+L_2)} \quad (7)$$
$$Z_3' = \frac{2Z_3}{n^4} \quad (8)$$
$$R' = \frac{2R}{n^4}. \quad (9)$$

The design parameters in (2) and (6)–(9) complete the transformation of the balun prototype of Fig. 2(b) into that of Fig. 5.

An effect way to increase the order of the Marchand balun is to add nonredundant UEs. Fig. 6 shows the S-plane high-pass prototype circuit of the N-order ($N \geqq 5$) Marchand balun.

III. Synthesis and Design of Two Balun Examples

A. Synthesis Procedures

Before designing the proposed balun, two important points should be addressed in the following. The first point is to determine a characteristic transfer function of the fifth-order Marchand balun. The second point is to apply the exact synthesis to the proposed balun such that the wideband responses can be predicted.

By observing the prototype circuit in Fig. 5, the suitable characteristic function exhibiting the Chebyshev responses, which is comprehensively discussed in [20], is given by

$$|K(S)|^2 = \varepsilon^2\left[T_m\left(\frac{S_C}{S}\right)T_n\left(\frac{\sqrt{1-S_C^2}}{\sqrt{1-S^2}}\right) - U_m\left(\frac{S_C}{S}\right)U_n\left(\frac{\sqrt{1-S_C^2}}{\sqrt{1-S^2}}\right)\right]^2 \quad (10)$$

where $S_C = j\tan(\pi f_C/2f_0)$, f_C is the filter cutoff frequency that is used to determine the bandwidth of the balun, ε specifies equal-ripple value, and $T_k(x)$ and $U_k(x)$ are the unnormalized Chebyshev polynomials of the first and second kinds of degree k, respectively. In (10), subscript m and n denote the number

of high-pass ladder elements (series capacitors and shunt inductors) and UEs, respectively.

Given $|K(S)|^2$, the square of the magnitude of the input reflection coefficient is obtained using

$$|S_{11}(S)|^2 = \frac{|K(S)|^2}{1+|K(S)|^2}. \tag{11}$$

$S_{11}(S)$ can then be found with the knowledge that

$$|S_{11}(S)|^2 = S_{11}(S)S_{11}(-S). \tag{12}$$

The relationship between input impedance $Z_{\text{in}}(S)$ and $S_{11}(S)$ with a normalized source resistance of 1 Ω is

$$Z_{\text{in}}(S) = \frac{1+S_{11}(S)}{1-S_{11}(S)}. \tag{13}$$

The circuit prototype to be synthesized is shown in Fig. 5. The first element to be extracted is the left-most UE of the circuit. By applying Richards' theorem, a UE can be obtained using

$$Z_{\text{UE},i}(S) = Z_{\text{in},i}(1) \tag{14}$$

where $Z_{\text{UE},i}$ denotes the impedance value of the ith UE and $Z_{\text{in},i}(1)$ is the input impedance looking from the ith UE. The input impedance of the remaining network after removal of the extracted UE is

$$Z'_{\text{in},i}(S) = Z_{\text{in},i}(1)\frac{SZ_{\text{in},i}(1) - Z_{\text{in}}(S)}{SZ_{\text{in}}(S) - Z_{\text{in},i}(1)} \tag{15}$$

where the common factor of S^2-1 can be cancelled out.

The second and third element types to be extracted are the series capacitor and shunt inductor. The method used to synthesize lumped-element ladder networks can be applied to this balun prototype and obtain the element values of the series capacitor and shunt inductor.

B. Two Design Examples

The two examples of fifth-order equal-ripple wideband Marchand baluns corresponding to the S-plane high-pass prototype, as shown in Fig. 5, are considered in this paper.

The first balun is designed with the center frequency f_0 of 2 GHz, a normalized cutoff frequency of $S_C = j0.6$ corresponding to a bandwidth of 131%, and a ripple level of $\varepsilon = 0.0945$ corresponding to a return loss of 20.53 dB. Applying these parameters into (10), the characteristic polynomial $|K(S)|^2$ can be constructed as

$$|K(S)|^2 = \frac{0.1965S^8+0.9304S^6+1.4332S^4+0.7855S^2+0.1400}{-S^{10}+3S^8-3S^6+S^4}. \tag{16}$$

The square of the magnitude of the input reflection coefficient is then established by (11), and with the knowledge of (12) it can lead to

$$S_{11}(S) = \frac{0.4433S^4+1.0496S^2+0.3743}{S^5+3.7102S^4+5.2847S^3+3.8768S^2+1.4545S+0.3741}. \tag{17}$$

The input impedance is then obtained by (13) as

$$Z_{\text{in}}(S) = \frac{S^5+4.1535S^4+5.2847S^3+4.9264S^2+1.4545S+0.7484}{S^5+3.2669S^4+5.2847S^3+2.8272S^2+1.4545S}. \tag{18}$$

The following step is to synthesize the element values in Fig. 5. To extract the encountered UE value and to obtain the input impedance of the remaining network, (14) and (15) are used. The standard synthesis procedure of lumped-element ladder networks is then applied to extract the series capacitor and shunt inductor. Thus, the circuit element values of the first balun with a normalized source resistance of 1 Ω are

$$\begin{aligned} Z_1 &= 1.27 \\ C &= 1.1561 \\ Z'_2 &= 1 \\ L' &= 1.1563 \\ Z'_3 &= 0.7871 \\ R' &= 1. \end{aligned} \tag{19}$$

Substituting (19) into (2) and (6)–(9) and de-normalizing to the 50-Ω system then gives the design parameters of Fig. 1 as follows:

$$\begin{aligned} Z_1 &= 63.5\,\Omega \\ Z_C &= 43.25\,\Omega \\ Z_{L1} &= 170.71\,\Omega \\ Z_2 &= 70.71\,\Omega \\ Z_{L2} &= 221.93\,\Omega \\ Z_3 &= 39.36\,\Omega. \end{aligned} \tag{20}$$

The second balun is with the center frequency f_0 of 2 GHz, a normalized cutoff frequency of $S_C = j0.4$ corresponding to a bandwidth of 152%, and ripple level $\varepsilon = 0.08243$ corresponding to a return loss of 21.71 dB. Similarly, follow the synthesized procedures, as described in the first designed balun. The polynomial of the input impedance, the circuit parameters corresponding to Fig. 5 in a normalized source resistance of 1 Ω, and the design parameters of Fig. 1 in the 50-Ω system are shown in (21)–(23), respectively,

$$Z_{\text{in}}(S) = \frac{S^5+3.7080S^4+4.1420S^3+2.7908S^2+0.5574S+0.1700}{S^5+3.0432S^4+4.1420S^3+1.8277S^2+0.5574S} \tag{21}$$

and

$$\begin{aligned} Z_1 &= 1.1701 \\ C &= 2.4243 \\ Z'_2 &= 1 \\ L' &= 2.4243 \\ Z'_3 &= 0.8546 \\ R' &= 1 \end{aligned} \tag{22}$$

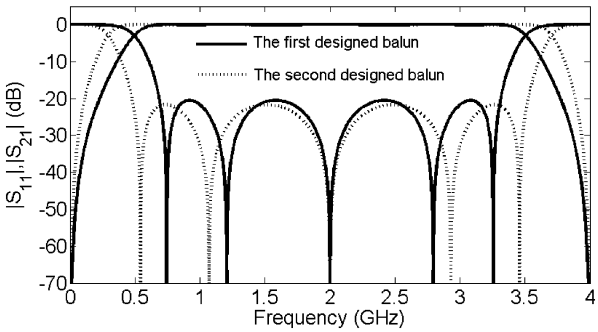

Fig. 7. Ideal responses of the first and second designed baluns with bandwidth of 131% and 152%, respectively.

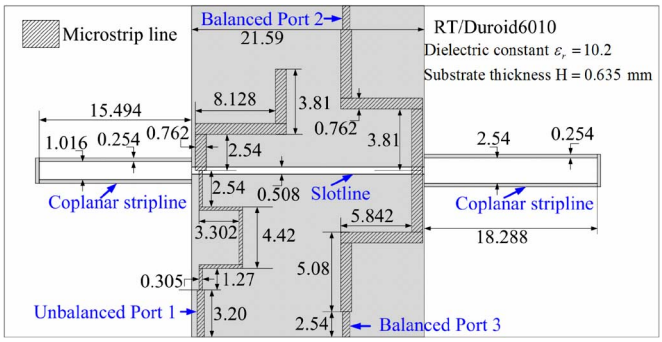

Fig. 8. Physical layout of the first designed fifth-order balun with $S_C = j0.6$ (unit: millimeters).

$$
\begin{aligned}
Z_1 &= 58.51\ \Omega \\
Z_C &= 20.62\ \Omega \\
Z_{L1} &= 170.71\ \Omega \\
Z_2 &= 70.71\Omega \\
Z_{L2} &\gg 377\ \Omega \\
Z_3 &= 42.73\ \Omega. \qquad (23)
\end{aligned}
$$

The ideal responses of the two designed baluns corresponding to the circuit of Fig. 5 are shown in Fig. 7.

IV. Physical Implementation and Experimental Results

The practical implementations of the two designed wideband baluns comprise the microstrip lines, slotlines, and coplanar striplines. A 0.635-mm-thick RT/Duroid6010 substrate with $\varepsilon_r = 10.2$ and a loss tangent of 0.0023 is used to implement the two wideband baluns. The distributed circuits to be directly realized are the circuit shown in Fig. 1. Here, the two short-circuit stubs Z_{L1} and Z_{L2}, the uniform transmission line Z_2, the open-circuit stub Z_C, and other uniform transmission lines Z_1 and Z_3 are implemented by coplanar striplines, a slotline, and microstrip lines, respectively. The microstrip lines (Z_1 and Z_3) are constructed on the front side, whereas the slotline (Z_2) and coplanar striplines are on the back side. Moreover, the slotline also serves as the ground plane of the microstrip lines. This arrangement not only saves the circuit area, but also provides the straightforward connection between coplanar striplines and slotlines. The coplanar striplines and slotline are both balanced transmission lines, which ensure the differential-mode signal transmission. All the stubs and uniform transmission line sections are with electrical lengths of 90° at the center frequency of $f_0 = 2$ GHz.

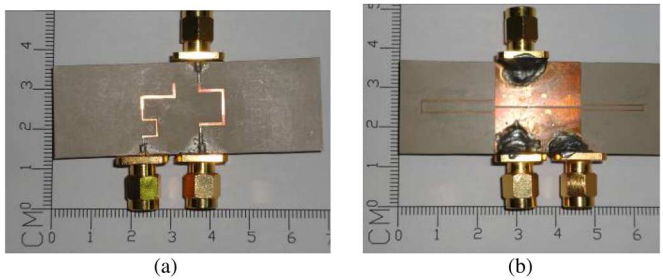

Fig. 9. Photograph of the first designed fifth-order balun. (a) Top view. (b) Bottom view.

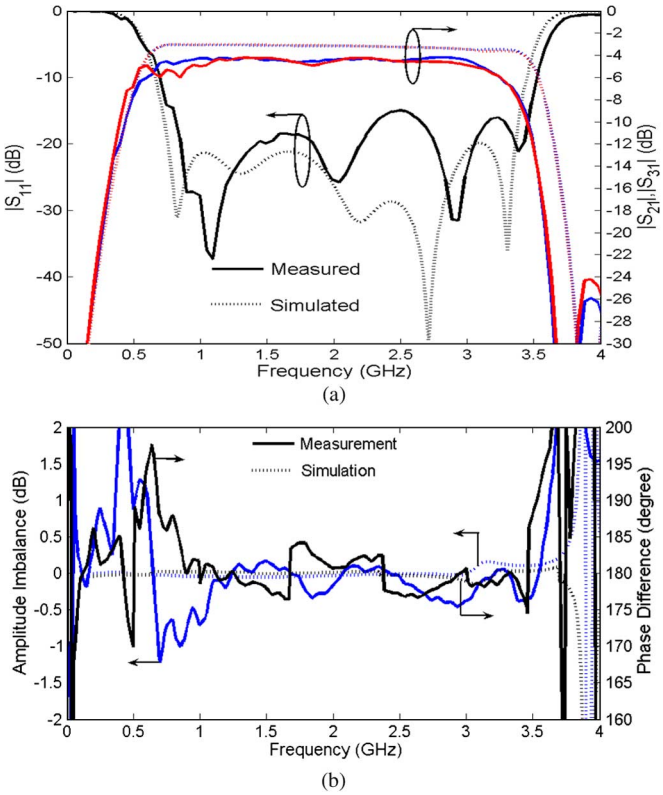

Fig. 10. Measured and simulated performances of the first fifth-order balun. (a) $|S_{11}|$, $|S_{21}|$, and $|S_{31}|$. (b) Amplitude imbalance and phase difference.

Fig. 8 depicts the detailed physical dimensions of the first balun. The design was accomplished with a commercial electromagnetic (EM) simulator, i.e., Ansoft's High Frequency Structure Simulator (HFSS). Fine tuning in HFSS was performed to take all the EM effects into consideration. The top- and bottom-view photographs of the fabricated first designed balun are shown in Fig. 9(a) and (b), respectively. The top-view photograph shows the realizations of the microstrip lines corresponding to the circuit elements Z_1, Z_C, and Z_3 in Fig. 1. While the bottom-view photograph shows the realizations of the two coplanar striplines and the slotline corresponding to the circuit elementsZ_{L1}, Z_{L2}, and Z_3, respectively, in Fig. 1. Fig. 10 shows the simulated and measured performances. The measured return losses are better than 10 dB from 0.7 to

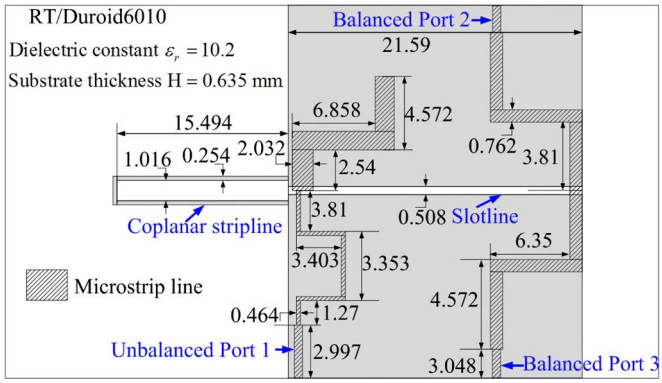

Fig. 11. Physical layout of the second designed fifth-order balun with $S_C = j0.4$ (unit: millimeters).

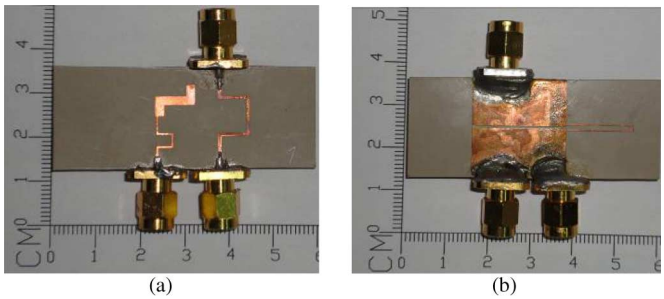

(a) (b)

Fig. 12. Photograph of the second designed fifth-order balun. (a) Top view. (b) Bottom view.

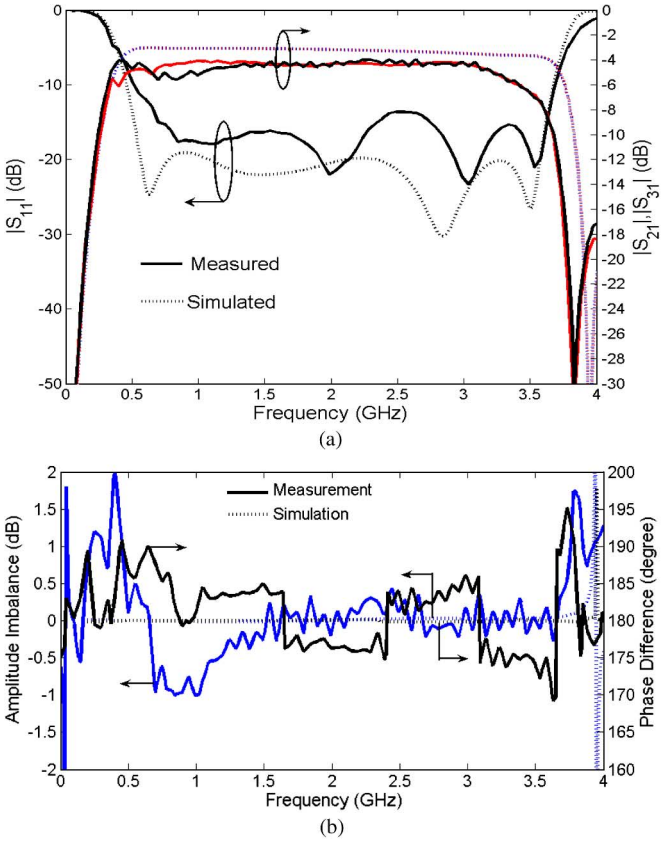

Fig. 13. Measured and simulated performances of the second fifth-order balun. (a) $|S_{11}|$, $|S_{21}|$, and $|S_{31}|$. (b) Amplitude imbalance and phase difference.

3.5 GHz. The measured amplitude imbalance is within ± 1 dB from 0.72 to 3.62 GHz and the measured phase difference is within $180^\circ \pm 10^\circ$ from 0.7 to 3.53 GHz.

The physical layout of the second balun is shown in Fig. 11. It should be pointed out that the synthesized impedance value of Z_{L2} is much larger than the intrinsic impedance in free space, which is equal to 377 Ω. Thus, the Z_{L2} section can be removed. The top- and bottom-view photographs of the fabricated second designed balun are shown in Fig. 12(a) and (b), respectively. The simulated and measured performances are shown in Fig. 13. The measured return losses are better than 10 dB from 0.52 to 3.68 GHz. The measured amplitude imbalance is within ± 1 dB from 0.46 to 3.75 GHz and the measured phase imbalance is within $180^\circ \pm 10^\circ$ from 0.46 to 3.62 GHz.

V. Conclusion

This paper has proposed a planar circuit Marchand balun structure. The novel circuit structure is suitable for the circuit synthesis of the Richard's domain high-pass prototype. Comparing to the conventional fourth-order Marchand balun, the proposed Marchand balun can easily implement a circuit with the order higher than five. The responses of the synthesized circuits are exact. Two fifth-order examples have been given to show the feasibility of the planar circuit implementation and their wideband performances.

References

[1] R. Mongia, I. Bahl, and P. Bhartia, *RF and Microwave Coupled-Line Circuits*. Norwood, MA: Artech House, 1999, pp. 391–442.

[2] A. M. Pavio and A. Kikel, "A monolithic or hybrid broadband compensated balun," in *IEEE MTT-S Int. Microw. Symp. Dig.*, May 1990, pp. 483–486.

[3] B. J. Minnis and M. Healy, "New broadband balun structures for monolithic microwave integrated circuits," in *IEEE MTT-S Int. Microw. Symp. Dig.*, Jun. 1991, pp. 425–428.

[4] K. S. Ang, Y. C. Leong, and C. H. Lee, "Multisection impedance-transforming coupled-line baluns," *IEEE Trans. Microw. Theory Tech.*, vol. 51, no. 2, pp. 536–541, Feb. 2003.

[5] D. Kuylenstierna and P. Linner, "Design of broadband lumped-element baluns with inherent impedance transformation," *IEEE Trans. Microw. Theory Tech.*, vol. 52, no. 12, pp. 2739–2745, Dec. 2004.

[6] N. Marchand, "Transmission line conversion transformers," *Electron*, vol. 17, no. 12, pp. 142–145, Dec. 1944.

[7] J. Cloete, "Exact design of the Marchand balun," *Microw. J.*, vol. 23, no. 5, pp. 99–102, May 1980.

[8] J. Cloete, "Graphs of circuit elements for the Marchand balun," *Microw. J.*, vol. 24, no. 5, pp. 125–128, May 1981.

[9] C. L. Goldsmith, A. Kikel, and N. L. Wilkens, "Synthesis of Marchand baluns using multilayer microstrip structures," *Int. J. Microw. Millimeter-Wave Comput.-Aided Eng.*, vol. 2, no. 3, pp. 179–188, 1992.

[10] K. S. Ang and I. D. Robertson, "Analysis and design of impedance-transforming planar Marchand baluns," *IEEE Trans. Microw. Theory Tech.*, vol. 49, no. 2, pp. 402–406, Feb. 2001.

[11] S. C. Tseng, C. C. Meng, C. H. Chang, C. K. Wu, and G. W. Huang, "Monolithic broadband Gilbert micromixer with an integrated Marchand balun using standard silicon IC process," *IEEE Trans. Microw. Theory Tech.*, vol. 54, no. 12, pp. 4362–4371, Dec. 2006.

[12] C. S. Lin, P. S. Wu, M. C. Yeh, J. S. Fu, H. Y. Chang, K. Y. Lin, and H. Wang, "Analysis of multiconductor coupled-line Marchand baluns for miniature MMIC design," *IEEE Trans. Microw. Theory Tech.*, vol. 55, no. 6, pp. 1190–1199, Jun. 2007.

[13] C. W. Tang and C. Y. Chang, "A semi-lumped balun fabricated by low temperature co-fired ceramic," in *IEEE MTT-S Int. Microw. Symp. Dig.*, Jun. 2002, pp. 2201–2204.

[14] M. J. Chiang, H. S. Wu, and C. K. Tzuang, "A compact CMOS Marchand balun incorporating meandered multilayer edge-coupled transmission lines," in *IEEE MTT-S Int. Microw. Symp. Dig.*, Jun. 2009, pp. 125–128.

[15] S. A. Maas, *The RF and Microwave Circuit Design Cookbook*. Norwood, MA: Artech House, 1998, pp. 109–114.
[16] Y. S. Lin and C. H. Chen, "Lumped-element Marcand-balun type coplanar waveguide-to-coplanar stripline transitions," in *Proc. Asia–Pacific Microw. Conf.*, Dec. 2001, pp. 539–542.
[17] W. M. Fathelbab and M. B. Steer, "New class of miniaturized planar Marchand baluns," *IEEE Trans. Microw. Theory Tech.*, vol. 53, no. 4, pp. 1211–1220, Apr. 2005.
[18] Z. Xu and L. MacEachern, "Optimum design of wideband compensated and uncompensated Marchand baluns with step transformers," *IEEE Trans. Microw. Theory Tech.*, vol. 57, no. 8, pp. 2064–2071, Aug. 2009.
[19] H. J. Orchard and G. C. Temes, "Filter design using transformed variable," *IEEE Trans. Circuit Theory*, vol. CT-15, no. 12, pp. 385–408, Dec. 1968.
[20] M. Horton and R. Wenzel, "General theory and design of optimum quarter-wave TEM filters," *IEEE Trans. Microw. Theory Tech.*, vol. MTT-13, no. 5, pp. 316–327, May 1965.
[21] D. M. Pozer, *Microwave Engineering*, 3rd ed. New York: Wiley, 2005, p. 407.

Jhe-Ching Lu was born in Kaohsiung, Taiwan, on May 18, 1982. He received the B.S. degree in electrical engineering from National Sun Yat-Sen University, Kaohsiung, Taiwan, in 2004, and M.S. and Ph.D. degrees in communication engineering from National Chiao-Tung University, Hsinchu, Taiwan, in 2006 and 2009, respectively.

In 2009, he joined the Taiwan Semiconductor Manufacture Company Ltd. (TSMC), Hsinchu, Taiwan. He is currently with the RF Modeling Program, TSMC. His research interests include the analysis and design of microwave and millimeter-wave circuits and RF device characterization and modeling.

Chung-Chieh Lin was born in Taipei, Taiwan. He received the B.S. degree in electrical engineering and M.S. degree in communication engineering from National Chiao-Tung University, Hsinchu, Taiwan, in 2007 and 2009, respectively.

His research interest is microwave passive component design.

Chi-Yang Chang (S'88–M'95) was born in Taipei, Taiwan, on December 20, 1954. He received the B.S. degree in physics and M.S. degree in electrical engineering from National Taiwan University, Taipei, Taiwan, in 1977 and 1982, respectively, and the Ph.D. degree in electrical engineering from The University of Texas at Austin, in 1990.

From 1979 to 1980, he was with the Department of Physics, National Taiwan University, as a Teaching Assistant. From 1982 to 1988, he was with the Chung-Shan Institute of Science and Technology (CSIST), as an Associate Researcher, where he was in charge of the development of microwave integrated circuits (MICs), microwave subsystems, and millimeter-wave waveguide E-plane circuits. From 1990 to 1995, he returned to CSIST, as an Associate Researcher in charge of the development of uniplanar circuits, ultra-broadband circuits, and millimeter-wave planar circuits. In 1995, he joined the faculty of the Department of Communication, National Chiao-Tung University, Hsinchu, Taiwan, as an Associate Professor and became a Professor in 2002. His research interests include microwave and millimeter-wave passive and active circuit design, planar miniaturized filter design, and monolithic-microwave integrated-circuit (MMIC) design.